

1 ***Xanthomonas oryzae* pv. *oryzae* type-III effector TAL9b targets a broadly conserved**
2 **disease susceptibility locus to promote pathogenesis in rice**

3
4 Gokulan C.G.^{1†}, Sohini Deb^{1,2‡}, Namami Gaur^{1,3†}, Apoorva Masade¹, Niranjan Gattu¹, Renny
5 P.R.¹, Nisha Sao¹, Donald James^{1,4}, Ramesh V. Sonti^{1,5,‡}, Hitendra K. Patel^{1,6,‡}
6

7 ¹Centre for Cellular and Molecular Biology (CSIR-CCMB), Hyderabad, India - 500007.

8 ⁵International Centre for Genetic Engineering and Biotechnology, New Delhi, India - 110067.

9 ⁶Academy of Scientific and Innovative Research, Ghaziabad, India - 201002.

10 [†] Equally contributed authors

11 [‡] Corresponding authors

12 **Addresses for correspondence:** Ramesh V. Sonti: sonti@icgeb.res.in; Hitendra K Patel:
13 hkpatel@ccmb.res.in

14
15 **Keywords:** Rice, *Xanthomonas*, Salicylic acid, Flavonoids, TAL effectors, Disease
16 susceptibility.

²Current address: Department of Plant and Environmental Sciences, Section for Plant and Soil Sciences, University of Copenhagen, Thorvaldsensvej 40, 1871 Frederiksberg C, Denmark.

³Current address: The James Hutton Institute, Invergowrie, DD2 5DA, Scotland, UK.

⁴Current address: Kerala Forest Research Institute, Peechi, India - 680653.

17 **SUMMARY**

18 *Xanthomonas oryzae* pv. *oryzae* (Xoo), the causal agent of bacterial blight of rice, translocates
19 multiple Transcription Activator-Like Effectors (TALEs) into rice cells. The TALEs localize
20 to the host cell nucleus, where they bind to the DNA in a sequence-specific manner and enhance
21 gene expression to promote disease susceptibility. Xoo strain PXO99^A encodes nineteen
22 TALEs, but the host targets of all these TALEs have not been defined. A meta-analysis of rice
23 transcriptome profiles revealed a gene annotated as flavonol synthase/flavanone-3 hydroxylase
24 (henceforth *OsS5H/FNS-03g*) to be highly induced upon Xoo infection. Further analyses
25 revealed that this gene is induced by PXO99^A using TAL9b, a broadly conserved TALE of
26 Xoo. Disruption of *tal9b* rendered PXO99^A less virulent. *OsS5H/FNS-03g* functionally
27 complemented its *Arabidopsis* homologue AtDMR6, a well-studied disease susceptibility
28 locus. Biochemical analyses suggested that *OsS5H/FNS-03g* is a bifunctional protein with
29 Salicylic Acid 5' Hydroxylase (S5H) and Flavone Synthase-I (FNS-I) activities. Further, an
30 exogenous application of apigenin on rice leaves, the flavone that is enzymatically produced
31 by *OsS5H/FNS-03g*, promoted virulence of PXO99^A *tal9b*-. Overall, our study suggests that
32 *OsS5H/FNS-03g* is a bifunctional enzyme and its product apigenin is potentially involved in
33 promoting Xoo virulence.

34

35 INTRODUCTION

36 Phytopathogens deploy several virulence factors to control host physiology and
37 promote pathogenesis (Wang and Wang, 2018). The genus *Xanthomonas* comprises several
38 economically important phytopathogens that cause severe yield losses in multiple important
39 food crops globally (White et al., 2009). *Oryza sativa* (henceforth rice) is an important food
40 crop that feeds about half of the global human population (Fukagawa and Ziska, 2019). Rice
41 production is hampered by multiple diseases, one of most devastating is the bacterial blight
42 (BB) disease caused by *Xanthomonas oryzae* pv. *oryzae* (Xoo; Savary et al., 2019). Yet another
43 bacterial disease of rice is bacterial leaf streak (BLS) caused by *X. oryzae* pv. *oryzicola* (Xoc).
44 Although Xoo and Xoc are pathovars of *X. oryzae*, their mode of infection and colonization in
45 rice leaves are different. Xoo, a vascular pathogen, enters through either hydathodes or wounds
46 and colonizes the xylem vessels. On the other hand, Xoc invades rice through stomata or
47 wounds and colonizes the mesophyll tissue (Niño-Liu et al., 2006). Both Xoo and Xoc utilize
48 the type III secretion system (T3SS) to deploy a specific class of effectors known as
49 Transcription Activator-Like Effectors (TALEs) directly into the rice cells to promote
50 pathogenesis (White et al., 2009).

51 TALEs consist of ~34 conserved repeating amino acids that vary at positions 12 and 13
52 in each repeat. These pairs of residues called Repeat Variable Diresidue (RVD) interact with
53 the Effector Binding Element (EBE) in the promoters of host target genes and modulate their
54 expression (Boch et al., 2009; Bogdanove et al., 2010). More often than not, the TAL effector
55 targeted host genes confer disease susceptibility and are known as susceptibility factors
56 (Antony et al., 2010; Cernadas et al., 2014; Peng et al., 2019; Streubel et al., 2013; Sugio et al.,
57 2007; Tran et al., 2018; Wu et al., 2022; Yang et al., 2006). Understanding the mechanisms of
58 TALE-mediated host susceptibility is important to devise strategies for disease resistance
59 breeding. For instance, certain Xoo-delivered TALEs recognize EBE in the genes encoding the

60 SUGARS WILL EVENTUALLY BE EXPORTED TRANSPORTER (SWEET) family
61 proteins and induce their expression to enhance apoplastic sucrose availability (Bezrutczyk et
62 al., 2018; Streubel et al., 2013). Interfering with the ability of Xoo to induce *SWEET* genes
63 makes the plants resistant to Xoo infection (Blanvillain-Baufumé et al., 2017; Chu et al., 2006;
64 Oliva et al., 2019). Further, Mücke et al., (2019) identified several rice genes that are directly
65 induced by Xoo TALEs. Besides the examples in Xoo, studies have also been conducted on
66 the role of TALEs in Xoc pathogenesis. For instance, severe water-soaked leaf streaking was
67 shown to be associated with $Tal2g_{BLS256}$ -dependent upregulation of a rice gene called
68 *OsSULTR3;6* (Cernadas et al., 2014). Another study reported that $Tal7_{RS105}$ activates the
69 promoters of two rice genes *Os09g29100* (predicted to encode Cyclin-D4-1) and *Os12g42970*
70 (predicted to encode a GATA zinc finger family protein), and that $Tal7_{RS105}$ suppresses *avrXa7-*
71 *Xa7* mediated defense in Rice (Cai et al., 2017).

72 A recent study identified a rice FLAVANONE 3' HYDROXYLASE encoding gene
73 (*OsF3H03g*; *LOC_Os03g03034*) to be targeted by Xoc in a TALE-dependent manner. Notably,
74 the presence of the cognate TALE that induces *OsF3H03g* correlated with the hypervirulence of
75 the tested Xoc strain (Wu et al., 2022). Earlier it was reported that the same gene (called *OsFNS*
76 therein) is induced by Xoo TALEs that belong to the class TAL AQ (that includes TAL9b in
77 Xoo PXO99^A) by introducing the TALE into an Xoo strain that lacks TAL effectors (Mücke et
78 al., 2019). Intriguingly, *OsF3H03g* is one of the very few genes that is induced by TALEs from
79 Xoo as well as Xoc (Cernadas et al., 2014; Mücke et al., 2019). *OsF3H03g* has been annotated
80 with various names in annotation servers and by different studies including 2-oxoglutarate
81 dependent dioxygenase (2-ODD/DOX), flavone synthase (FNS), flavanone 3' hydroxylase
82 (F3H), and salicylic acid (SA) 5' hydroxylase (S5H). Two recent studies reported that
83 *OsF3H03g* catalyses SA 5' hydroxylation to form 2,5-dihydroxybenzoic acid (2,5-DHBA) and
84 established that mutating rice S5Hs resulted in broad-spectrum disease resistance (Liu et al.,

85 2023; Zhang et al., 2022). On the other hand, an earlier study showed the FNS activity of
86 OsF3H_{03g} (Kim et al., 2008). However, no study has formally shown that purified OsF3H_{03g} is
87 a bifunctional protein that possesses both FNS and S5H biochemical activities. This lack of
88 clarity on the activity of OsF3H_{03g} has been previously highlighted (Mücke et al., 2019; Wu et
89 al., 2022).

90 Here, we validated the predicted role of TAL9b in inducing *OsF3H_{03g}* and showed that
91 the disruption of *tal9b* compromised the virulence of PXO99^A. Ectopic expression of
92 *OsF3H_{03g}* in *Arabidopsis atdmr6* mutant plants restored susceptibility of the plants to
93 *Pseudomonas syringae* pv. *tomato* DC3000, indicating that OsF3H_{03g} is a functional
94 homologue of *Arabidopsis* DOWNY MILDEW RESISTANT 6 (DMR6). Biochemical assays
95 using purified recombinant protein indicated that the protein performs dual functions *in vitro*
96 i.e., SA hydroxylation and flavone synthesis. Therefore, we address the protein henceforth as
97 OsS5H/FNS-03g. Furthermore, we identified a virulence promoting activity of the flavone
98 apigenin - enzymatically produced by OsS5H/FNS-03g - wherein it enhanced the virulence
99 of the PXO99^A *tal9b*- strain. Overall, our study expands the bacterial blight susceptibility
100 gene repertoire of rice and reinforces that DMR6 homologues are an evolutionarily conserved
101 plant disease susceptibility hub and are a potential target for disease resistance breeding in
102 various crops.

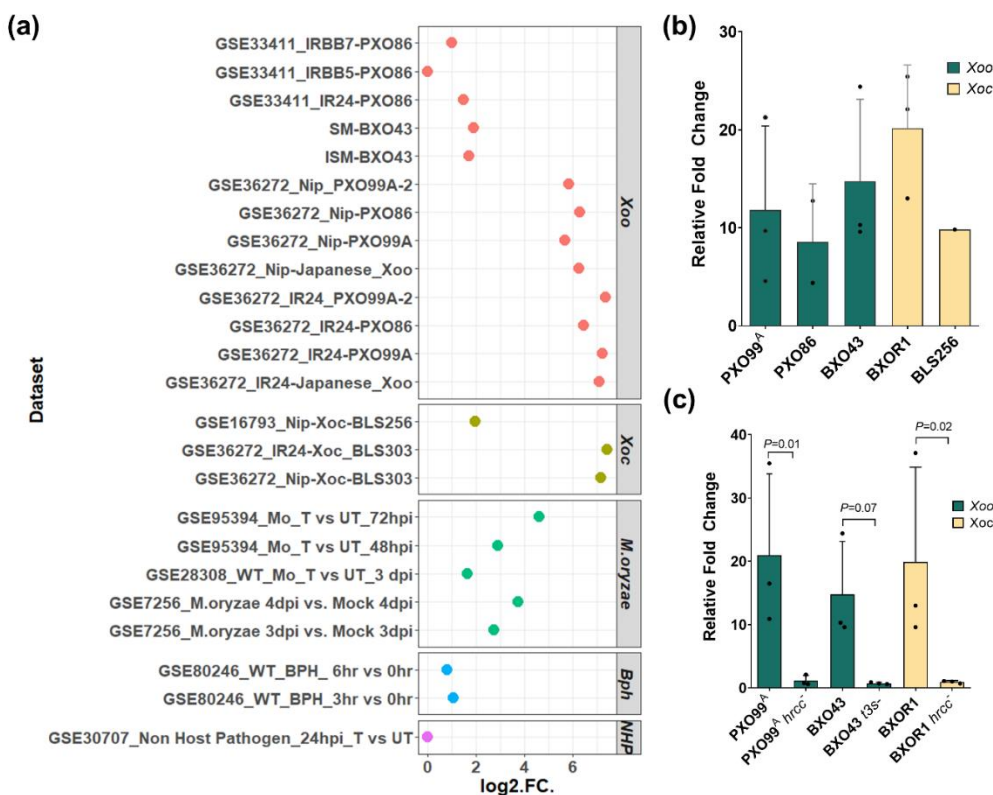
103

104 **RESULTS**

105 **The rice gene *LOC_Os03g03034* is induced by multiple pathogens and pests**

106 Analysis of publicly available gene expression data (Table S1) revealed that the rice
107 gene *LOC_Os03g03034* is highly induced by *Xanthomonas oryzae* pv. *oryzae*, *Xanthomonas*
108 *oryzae* pv. *oryzicola*, *Magnaporthe oryzae*, and infestation by the brown plant hopper
109 (*Nilaparvata lugens*) insect pest but not by a non-host pathogen *Puccinia triticina* f. sp. *tritici*
110 (Figure 1a). Semi-quantitative PCR analyses indicated that the transcript variant
111 *LOC_Os03g03034.1* is primarily induced by the tested strains (Figure S1) and thus has been
112 used throughout this study. Data mining from a public RNA-seq database revealed that the
113 expression of *OsS5H/FNS-03g* is induced primarily in pathogenic interactions as compared to
114 beneficial interactions (Figure S2a). Notably, induction of the gene, on average, was higher
115 during shoot/foliar pathogenesis (Figure S2b). We found that multiple strains of the *X. oryzae*
116 pathovars considerably induce the expression of *OsS5H/FNS-03g* (Figure 1b). We further
117 observed that the expression of *OsS5H/FNS-03g* increases temporally during Xoo infection of
118 rice (Figure S3a). Previous studies have reported that *OsS5H/FNS-03g* could be a target of Xoo
119 and Xoc type III- secreted TAL effectors. To validate the prediction, we generated the mutants
120 of Xoo PXO99^A and Xoc BXOR1 that are defective in the type III secretion system (T3SS).
121 Treatment of rice leaves with wild-type and T3SS mutant strains of both Xoo and Xoc showed
122 that the induction of *OsS5H/FNS-03g* is dependent on functional T3SS (Figure 1c). Taken

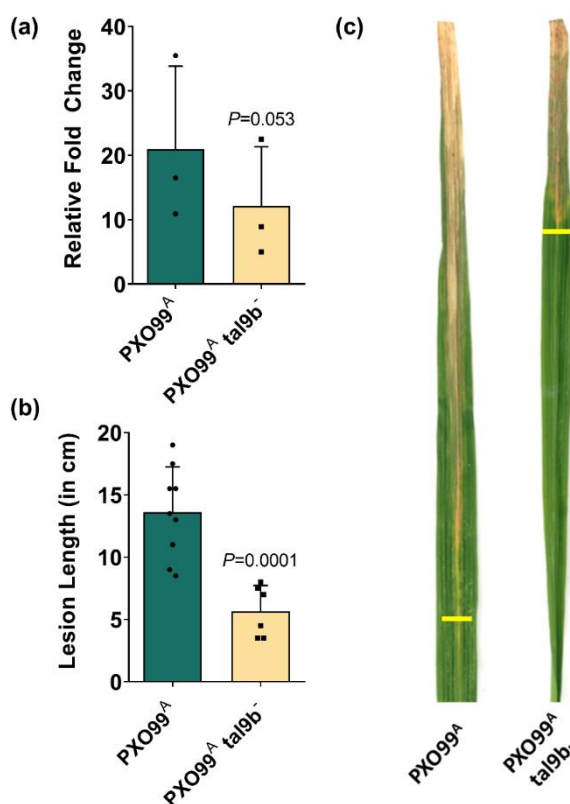
123 together, the results suggest that *OsS5H/FNS-03g* is a potential susceptibility gene to multiple
124 shoot/foliar pathogens and pests of rice.



125 **Figure 1: Expression of *OsS5H/FNS-03g* is highly induced during infection by various**
126 **pathogens and a pest.** (a) Various publicly available transcriptomics data were analysed and
127 *OsS5H/FNS-03g* was observed to be highly induced in pathogenic interactions of rice. Publicly
128 available microarray data were retrieved from NCBI-Gene Expression Omnibus and analysed
129 further to obtain the fold change values upon treatment as compared to the corresponding mock
130 treated samples. (b, c) Bacterial suspensions of indicated strains were infiltrated into the leaves
131 of 14-day old rice leaves, sampled at 24 hours post infiltration and the gene expression was
132 analysed using qRT-PCR. The gene expression levels were normalised with the internal control
133 *OsGAPDH*. Fold change values were calculated using the $2^{-\Delta\Delta C_t}$ method relative to the mock-
134 infiltrated samples. Error bars in (b) and (c) indicate the standard deviation of the fold change
135 values in a minimum of two independent experiments. *P* values were calculated using the One-
136 way ANOVA test.

137 **Disruption of TAL9b affects *OsS5H/FNS-03g* induction and virulence of Xoo PXO99^A**

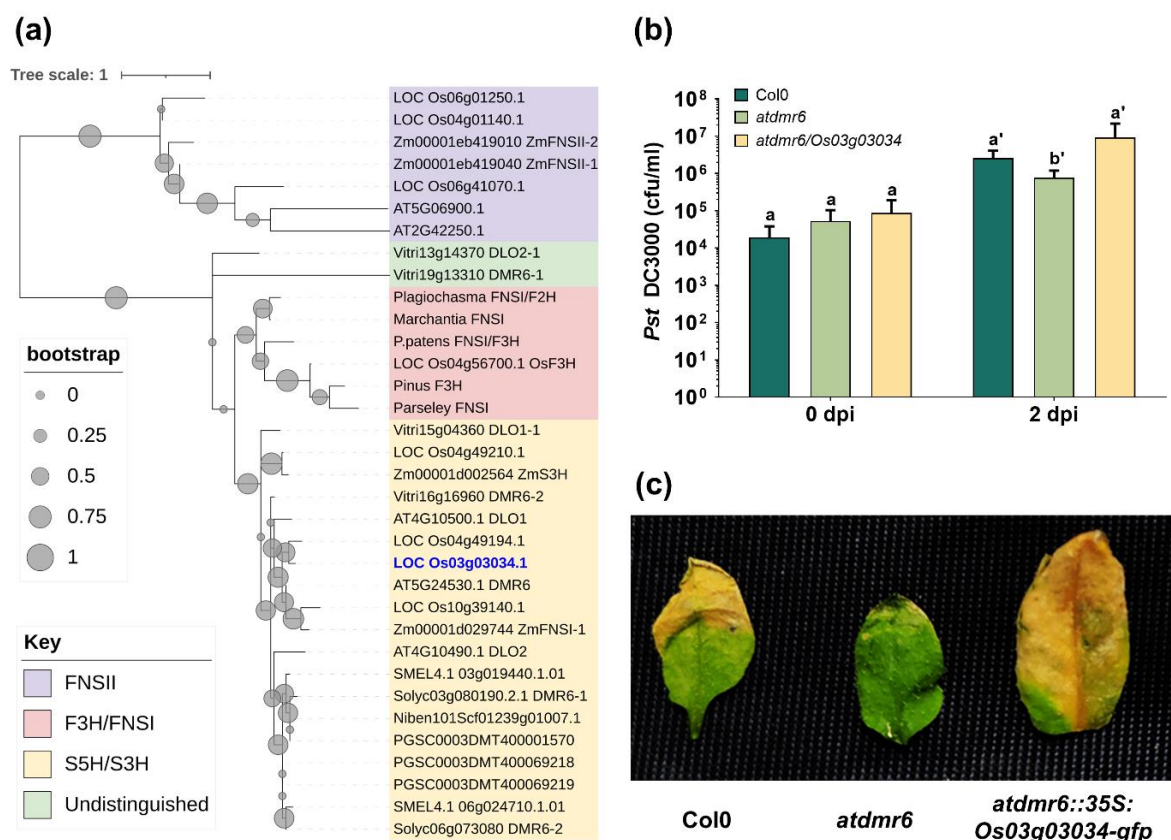
138 Previous reports indicated the presence of an EBE in the promoter of *OsS5H/FNS-03g*
139 (Cernadas et al., 2014; Mücke et al., 2019); Figure S4). Intriguingly, effectors from both the
140 pathovars of *X. oryzae* i.e., Xoo, and Xoc, utilise TALEs of different families to induce the
141 expression of *OsS5H/FNS-03g* while binding to the same EBE (Mücke et al., 2019; Figure S5).
142 *In silico* prediction analysis indicated that TAL9b encoded by Xoo PXO99^A is likely the
143 cognate TALE that activates the expression of *OsS5H/FNS-03g*. Therefore, a Tal9b-defective
144 mutant of Xoo PXO99^A (PXO99^A tal9b-) was generated through insertional mutagenesis to
145 study the role of TAL9b in *OsS5H/FNS-03g* induction and virulence of Xoo. Treatment of rice
146 leaves with PXO99^A tal9b- exhibited a reduced induction of *OsS5H/FNS-03g* transcripts when
147 compared to induction by the wild-type strain (Figure 2a). Further, the Tal9b mutant showed
148 significantly reduced virulence when compared to the wild-type strain on a susceptible rice line
149 (Figure 2b, c). These results indicate that optimal induction of *OsS5H/FNS-03g* by TAL9b is
150 required for full virulence of Xoo PXO99^A.



151 **Figure 2: Tal9b is required for induction of *OsS5H/FNS-03G* and full virulence of Xoo**
152 **PXO99^A.** (a) Gene expression analysis using qRT-PCR showed a reduced induction of
153 *OsS5H/FNS-03g* transcripts by the *Tal9b* mutant of Xoo PXO99^A. The gene expression
154 quantification was performed from leaf samples at 24 hours post infiltrating a suspension of
155 the described Xoo strains of OD_{600nm}=1 into the leaves of 14-day old TN1 rice plants. Error
156 bars indicate the standard deviation of the fold change values obtained with respect to the
157 mock-treated samples in three independent experiments. *P*-value was calculated using a two-
158 tailed paired *t* test. (b) Rice plants when 60 days old, were clip inoculated with PXO99^A and
159 PXO99^A *tal9b*- strains of OD_{600nm}=1. Bars in (b) indicate the average lesion length (n≥6) at 14-
160 days post infection (dpi) and the error bars represent the standard deviation. The *P*-value was
161 calculated using a two-tailed unpaired *t* test. Similar observations were made in multiple
162 independent experiments (n=3). (c) Lesion progression in representative leaves upon treatment
163 with the strains mentioned therein at 14 dpi. The yellow horizontal lines mark the leading edge
164 of the disease lesion.

165 **OsS5H/FNS-03g functionally complements its *Arabidopsis* homologue AtDMR6**

166 Protein sequence analysis revealed that OsS5H/FNS-03g is homologous to an
167 *Arabidopsis thaliana* protein called DOWNY MILDEW RESISTANT 6 (AtDMR6; Figure
168 3a). AtDMR6 has been characterised as a susceptibility factor for multiple pathogens including
169 *Hyaloperonospora parasitica* (downy mildew; oomycete), *Phytophthora capsica* (an
170 oomycete pathogen), *Pseudomonas syringae* pv. *tomato* DC3000 (*Pst* DC3000; bacterial
171 pathogen) (Zhang et al., 2017). To determine whether OsS5H/FNS-03g shares functional
172 homology with AtDMR6, an *Arabidopsis thaliana* line lacking *AtDMR6* gene (*atdmr6*) was
173 transformed with a construct carrying 35S:OsS5H/FNS-03g-GFP. Further, the transgenic
174 plants in T₂ generation, the *atdmr6* mutant, and the wild-type line (Col0) were inoculated with
175 the bacterial pathogen *Pst* DC3000, and bacterial growth was scored subsequently at 2dpi. It
176 was observed that ectopic expression of *OsS5H/FNS-03g* in *atdmr6* restored the susceptibility
177 to *Pst* DC3000 (Figure 3b, c) indicating a functional homology between OsS5H/FNS-03g and
178 AtDMR6 *in planta*.



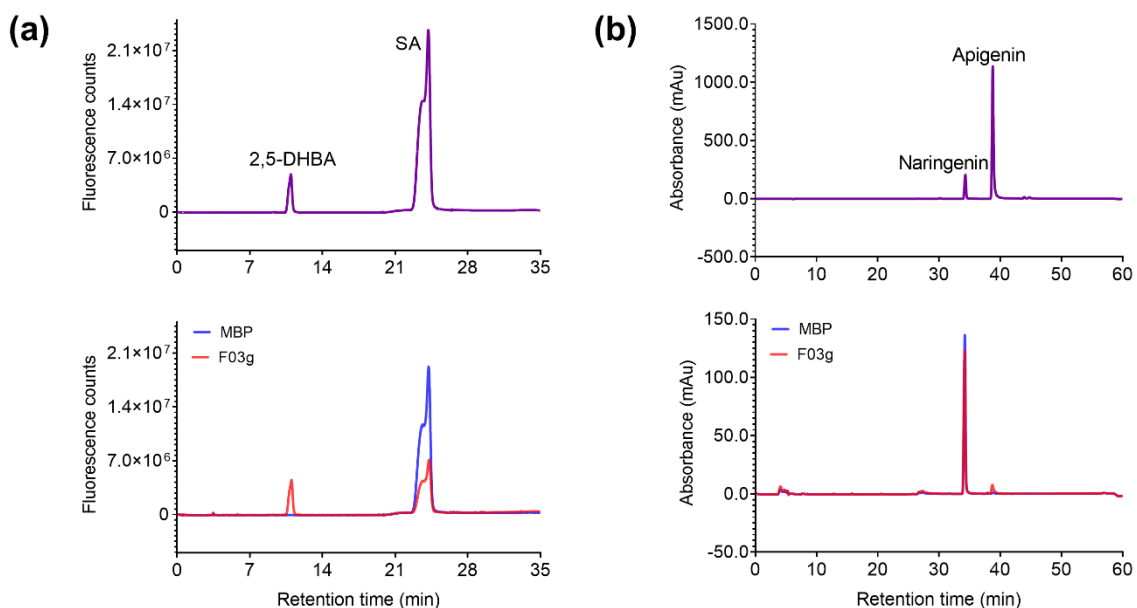
179 **Figure 3: OsS5H/FNS-03g complements AtDMR6 function in *Arabidopsis thaliana*.** (a) A
180 neighbourhood-joining based dendrogram indicating the sequence homology between various
181 orthologues of OsS5H/FNS-03g (in blue font). Protein sequences of the indicated species were
182 retrieved from literature information or by protein BLAST using OsS5H/FNS-03g sequence as
183 query. The clades are coloured based on the protein functions (b) Rosette leaves of wildtype
184 *Arabidopsis thaliana* Col0, *atdmr6* mutant, and transgenic *atdmr6* ectopically expressing
185 *OsS5H/FNS-03g-GFP* were syringe infiltrated with *Pst* DC3000 of OD_{600nm}=0.02. Bacterial
186 growth after 2 days of infiltration was determined by serial dilution plating on King's B agar
187 plates. (c) Disease symptoms on the infected leaves at 5 dpi. Bars in (b) represent the mean
188 colony forming units and the error bars indicate standard deviations in at least 3 biological
189 replicates. Bars capped with different alphabets indicate significant differences at a confidence
190 limit of 95% using Student's *t*-test. Similar results were obtained in three independent
191 experiments.

192

193 **OsS5H/FNS-03g is a bifunctional protein with S5H and FNS activities**

194 Complementation analysis confirmed that OsS5H/FNS-03g is a functional homologue
195 of AtDMR6. AtDMR6 is an SA hydroxylase that hydroxylates SA at the 5' position resulting
196 in the formation of 2,5 dihydroxybenzoic acid (2,5 DHBA) (Zeilmaker et al., 2015).
197 OsS5H/FNS-03g was reported by independent studies to have either S5H or FNS activities
198 (Kim et al., 2008; Liu et al., 2023; Zhang et al., 2022). Therefore, we investigated whether the
199 protein possesses both S5H and FNS activities. To this end, we expressed recombinant
200 OsS5H/FNS-03g that is N-terminally fused to Maltose Binding Protein (MBP) in *Escherichia*
201 *coli* and purified the protein using amylose resin. The purified protein preparation was used to
202 perform biochemical reactions to test the enzymatic function using SA and Naringenin as
203 substrates in independent reaction conditions. Purified MBP was used as a negative control.
204 Results show that OsS5H/FNS-03g efficiently catalyses SA hydroxylation at the 5' position
205 thereby producing 2,5-DHBA (Figure 4a). Further, the protein was also found to possess FNS
206 activity which was observed as a peak corresponding to the retention time of Apigenin standard
207 (Figure 4b). To confirm if the actual product is produced, the fraction corresponding to
208 apigenin retention time was collected from the standard, MBP control-, and MBP-
209 OsS5H/FNS-03g-containing reactions to analyse the product using Matrix-Assisted Laser
210 Desorption/Ionisation Time-Of-Flight (MALDI-TOF). The MALDI spectrum revealed a peak
211 with a mass-to-charge (m/z) ratio corresponding to apigenin (m/z = 271; including 1 Da added
212 by positive mode ionization) in standard and MBP-OsS5H/FNS-03g, and not in MBP control
213 sample (Figure S6). The results here suggest that OsS5H/FNS-03g possesses S5H as well as
214 FNS-I activities. Additionally, we noted that SA and Naringenin induce the expression of
215 *OsS5H/FNS-03g* to varied extents (Figure S3b).

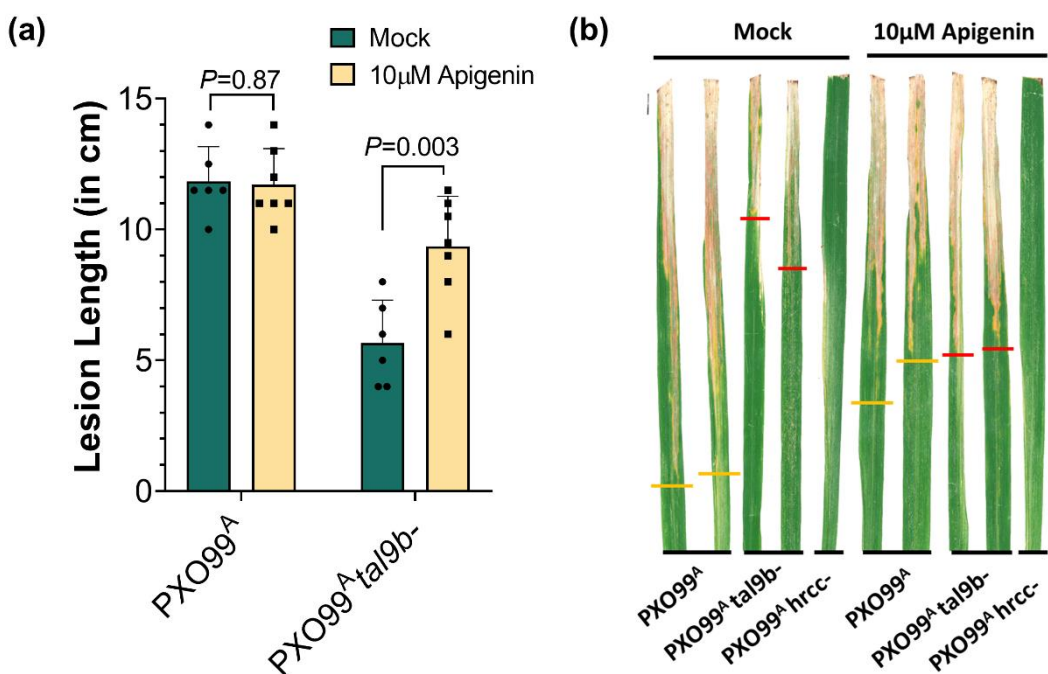
216



217 **Figure 4: OsS5H/FNS-03g is a bifunctional protein.** Chromatograms showing the authentic
218 standards (top) and reaction mixtures of MBP-OsS5H/FNS-03g (F03g) and MBP when
219 incubated with (a) SA and (b) Naringenin. The reactions were performed for one hour at
220 appropriate temperature and reaction conditions. The reaction mixture and authentic standards
221 were resolved further using High Performance Liquid Chromatography to observe the product
222 formation.

223 **Apigenin promotes virulence of PXO99^A *tal9b*-**

224 As OsS5H/FNS-03g catalysed the formation of apigenin, we asked if apigenin plays
225 any role in virulence of Xoo. For this, we exogenously applied 10 μ M apigenin by spraying on
226 rice leaves and subsequently infected the leaves with PXO99^A and PXO99^A *tal9b*- (24 hours
227 post spraying). Interestingly, we observed that prior application of apigenin enhanced the
228 virulence of the PXO99^A *tal9b*- and did not affect the virulence of PXO99^A (Figure 5a, b).
229 These results indicate that apigenin promotes the virulence of an otherwise less virulent mutant
230 of Xoo, which is also less proficient in inducing the expression of *OsS5H/FNS-03g*.



231 **Figure 5: Apigenin promotes virulence of PXO99^A tal9b⁻.** (a) TN1 rice leaves were sprayed
232 with either mock or 10µM apigenin to run off and were infected with the Xoo strains PXO99^A
233 and PXO99^A tal9b⁻ at 24 hours post spraying. Lesion lengths were measured at 14 dpi and the
234 mean length is represented as bars while the error bars indicate the standard deviation of the
235 lesion length in at least 6 infected leaves from one experimental replicate. The *P*-value was
236 calculated using an unpaired Student's *t*-test. The experiment was repeated twice with similar
237 observations. (b) The appearance of lesions in the infected leaves at 14 dpi. Yellow and red
238 lines on the leaves mark the tip of the lesion caused by PXO99^A and PXO99^A tal9b⁻,
239 respectively.

240

241 **DISCUSSION**

242 The Xoo pathogen deploys a sophisticated class of type III effector proteins called the
243 TAL effectors to take direct control on the transcription of certain host genes. Several host
244 genes that are activated in a TALE-dependent manner are reported to be *bona fide* susceptibility
245 factors (Boch et al., 2009; Streubel et al., 2013; Tran et al., 2018). Such TALEs are required
246 for full virulence of the pathogen. The Xoo strain PXO99^A encodes 19 TALEs in its genome
247 (Salzberg et al., 2008).

248 Here we report the identification and characterization of *OsS5H/FNS-03g* - a
249 bifunctional protein-coding gene that is activated by the PXO99^A TALE TAL9b. We observed
250 that *OsS5H/FNS-03g* is a functional homologue of the *Arabidopsis thaliana* DOWNY
251 MILDEW RESISTANT 6 (AtDMR6) protein. Accumulating evidence indicate that AtDMR6
252 and its orthologues are disease susceptibility factors for various pathogens in a wide variety of
253 plant species including *A. thaliana*, tomato, grapevine, maize, rice, and sweet basil (Djennane
254 et al., 2023; Falcone Ferreyra et al., 2015; Hasley et al., 2021; Liu et al., 2023; Pirrello et al.,
255 2022; Thomazella et al., 2021; Van Damme et al., 2008; Wu et al., 2022; Zeilmaker et al.,
256 2015; Zhang et al., 2022; Zhu et al., 2020). Biochemically, DMR6 orthologues catabolise
257 Salicylic acid (Thomazella et al., 2021; Zhang et al., 2017). Therefore, it is evident that several
258 evolutionarily distant pathogens with different modes of infection, convergently mediate SA
259 catabolism. This manipulation leads to a reduction in the *in planta* levels of SA, thereby
260 diminishing host immunity and possibly systemic acquired resistance.

261 **Possible role of flavones in disease susceptibility**

262 *OsS5H/FNS-03g* was first reported as a Flavone Synthase I (FNSI) that catalyses the
263 formation of the flavone apigenin using the flavanone naringenin as substrate (Kim et al.,
264 2008). As seen in Figure 3, S5H, FNS, and F3H proteins share high sequence homology. In
265 addition, neofunctionalization and dual activities of several F3H homologous proteins have

266 been reported by previous studies in various plant species (Li et al., 2020; Pucker and Iorizzo,
267 2023). Supporting (Falcone Ferreyra et al., 2015) and contradicting (Thomazella et al., 2021)
268 evidences exist regarding AtDMR6 and its FNS activity. Here, using the same protein
269 preparation, we showed that OsS5H/FNS-03g possesses both S5H and FNS activities *in vitro*.
270 Further, while testing the possible role of apigenin in plant susceptibility to Xoo, we observed
271 that apigenin promoted virulence of PXO99^A *tal9b*-, a strain that is otherwise less virulent and
272 defective in inducing *OsS5H/FNS-03g*.

273 Apigenin is known to serve multiple functions including the protection of plants from
274 Ultraviolet B (UV-B) radiation-induced damages (Righini et al., 2019), enhanced nutritional
275 value (Casas et al., 2014), enhanced tolerance to nitrogen deprivation through microbiome
276 modulation (Yu et al., 2021), enhanced biofilm formation by soil diazotrophic bacteria (Yan et
277 al., 2022), and a putative role in senescence (Falcone Ferreyra et al., 2015). Apigenin is also
278 known as a potent inducer of *nod* genes in *Sinorhizobium meliloti* (Peters et al., 1986; Watson
279 et al., 2015). In a similar manner, apigenin may induce expression of Xoo genes that are
280 involved in interaction with rice. Specifically, as in diazotrophs, apigenin may promote biofilm
281 formation of Xoo and thus enhance virulence. Furthermore, accumulation of apigenin beyond
282 a certain level during infection may also have a role in promoting senescence in leaves and
283 thus, enhance symptom formation. As can be seen, the literature suggests multiple possibilities
284 by which apigenin can promote virulence of Xoo, and additional studies are needed to
285 distinguish these various possibilities.

286 Yet another functional aspect of Xoo-mediated upregulation of an FNS activity-
287 containing protein could be to reduce the basal levels of the flavanone naringenin. It has been
288 reported that naringenin inhibits the growth of *X. oryzae* *in vitro* (Padmavati et al., 1997).
289 Further, the accumulation of naringenin was shown to provide broad-spectrum resistance to
290 rice pests (Yang et al., 2021). Additionally, naringenin was found to possess antimicrobial and

291 defense-inducing properties in other plant species like tobacco and *Arabidopsis* (An et al.,
292 2021; Shi et al., 2024; Sun et al., 2022). Therefore, it can be speculated that reducing the basal
293 level of naringenin during pathogenesis, possibly mediated by the induction of *OsS5H/FNS-*
294 *03g* will aid in rendering the host environment conducive for pathogen growth.

295 **OsS5H/FNS-03g is convergently targeted by diverse rice pathogens**

296 Xoo TALEs that target *OsS5H/FNS-03g* are present in most of the sequenced strains
297 (Figure S4). Intriguingly, *OsS5H/FNS-03g* is one of the few rice genes that is targeted by
298 TALEs from both the *X. oryzae* pathovars (Xoo and Xoc) by binding to the same effector
299 binding element (Cernadas et al., 2014; Mücke et al., 2019). Mücke et al., (2019) discussed the
300 convergence in the virulence mechanisms of the two *X. oryzae* pathovars and the plant
301 resistance mechanisms at *OsS5H/FNS-03g* and further called it a hub in the plant-pathogen
302 network. The observation that Xoo and Xoc pathovars are convergently targeting *OsS5H/FNS-*
303 *03g* denotes the existence of pathogenicity mechanisms that function beyond the tissue
304 specificity of the pathogens. That is, there exist certain susceptibility mechanisms that are
305 central to pathogenesis irrespective of the infection style and tissue specificity of the infecting
306 pathogen. This is further substantiated by the observation that the expression of *OsS5H/FNS-*
307 *03g* is induced by rice pathogens from different kingdoms (Figure S2). Identifying and
308 characterizing such broad-spectrum disease susceptibility factors will inform us of targets for
309 highly durable disease resistance breeding.

310 Overall, our study suggests that the flavone apigenin might play some important roles
311 in determining the outcomes of plant-pathogen interaction. Future studies directed towards
312 understanding the *in planta* and in bacteria role of apigenin are hence required. Also, the
313 disruption of EBE in the upstream sequence of *OsS5H/FNS-03g* through genome editing
314 approaches and pyramiding the disrupted EBE with other widely used resistance alleles can be
315 explored for developing broad spectrum resistance to Xoo.

317 **EXPERIMENTAL PROCEDURES**

318 **Plant, bacterial materials, and growth conditions**

319 The rice variety Taichung Native 1 (TN1), which is susceptible to bacterial blight
320 disease, was used for gene expression analysis and Xoo virulence assays. The seeds were
321 washed, soaked, and germinated on a moist filter paper and grown on Petri plates for 7 days.
322 Later, the seedlings were transplanted to pots containing black soil and grown for 7 more days
323 for gene expression analysis or were transplanted to the field until they were 60-days old for
324 performing virulence assays. All the experiments concerning TN1 were performed in green
325 house conditions with temperature not exceeding 30°C with 12 hour:12 hour light: dark cycles
326 and natural light conditions. *Arabidopsis thaliana* wildtype accession Columbia-0 (Col-0) and
327 the T-DNA insertion mutant line *atdmr6* (NASC ID: SK19087) were germinated on one-
328 strength Murashige-Skoog Agar medium with 2% sucrose and 0.8% agar at 22°C/18°C and
329 16h light/8h dark cycles. *atdmr6* lines were selected on plates containing an appropriate amount
330 of phosphinothricin. *Arabidopsis* seedlings were grown in a plant growth chamber (AR-75L3,
331 Percival-Scientific, USA) at 22°C/18°C at 16h light/8h dark cycles in pots containing 1:1:1
332 ratio of perlite: vermiculite: soilrite C (Keltech Energies, India).

333 Bacterial strains used in this study include *Escherichia coli* DH5α, S17-1 and Rosetta
334 DE3, *Agrobacterium tumefaciens* AGL1, *Xanthomonas oryzae* pv. *oryzae* PXO99^A, PXO86
335 and BXO43, *X. o.* pv. *oryzicola* BLS256 and BXORI, and *Pseudomonas syringae* pv. *tomato*
336 DC3000. *E. coli* strains were grown on Luria Bertani medium (10g/L peptone, 5g/l yeast
337 extract, 10g/L sodium chloride, pH 7.0); *Agrobacterium* strains were cultured on Yeast Extract
338 Mannitol medium (1g/L yeast extract, 10g/L Mannitol, 0.5g/L dipotassium phosphate, 0.2g/L
339 magnesium sulphate, 0.1g/L sodium chloride, pH 7.0); Xoo and Xoc were cultured on PS
340 medium (1% peptone and 1% sucrose, pH 7.0); Pst DC3000 was cultured in King's B medium.
341 *E. coli* was cultured at 37°C while the other bacteria were grown at 28°C. Appropriate

342 antibiotics/selection markers were used at the following concentrations: Rifampicin 50 μ g/ml,
343 Kanamycin 50 μ g/ml, Carbenicillin 50 μ g/ml, Chloramphenicol 30 μ g/ml, Spectinomycin
344 50 μ g/ml, Phosphinothricin (Basta) 20 μ g/ml, Hygromycin 25 μ g/ml. All the bacterial strains,
345 plant materials and plasmids used in this study are listed in Table S1.

346 **Analysis of public transcriptome data**

347 Publicly available Affymetrix microarray data pertinent to the interaction between rice
348 and its biotic stress factors with appropriate controls were retrieved from the NCBI-Gene
349 Expression Omnibus (GEO) repository (Table S2). The data were normalised and analysed
350 using Affymetrix Expression Console and Transcriptome Analysis Console. All the datasets
351 were normalised using the PLIER algorithm and further analysed to identify the differentially
352 expressed genes ($|FC| \geq 1.5$ and $P\text{-value} \leq 0.05$). The fold change values of *LOC_Os03g03034*
353 were retrieved by searching for the probe ID of the gene: Os.10510.1.S1_at and plotted in R-
354 studio using the *ggplot2* library. The expression level (FPKM) of *LOC_Os03g03034* under
355 various biotic stresses was retrieved from the Rice RNA-seq database
356 [<http://ipf.sustech.edu.cn/pub/ricerna/>; (Zhang et al., 2020)] and further processed and plotted
357 using Microsoft Excel and GraphPad Prism 8, respectively.

358 **Generation of mutant strains of Xoo and Xoc**

359 To generate the type-3 secretion system deficient strains of Xoo and Xoc, a 506bp long
360 segment of the *hrcC* gene was amplified from the genomic DNA of Xoo PXO99^A and Xoc
361 BXORI and cloned between the EcoRI and BamHI sites of the mobilizable vector pK18mob,
362 which upon integration into the bacterial genome, disrupts the gene and confers the cells
363 Kanamycin resistance. The plasmid DNA were sequence confirmed and used to transform the
364 *E. coli* strain S17-1. Further a biparental mating was set between *E. coli* S17-1 carrying the
365 plasmid of interest and the Xoo/Xoc strains at a ratio of 1:5, 1:15, and 1:25 of *E. coli* to
366 Xoo/Xoc for 48-72 hours on autoclaved nylon membranes at 28°C. The cells were scraped and

367 plated on PS plates containing Kanamycin to select the integrants. The integration was
368 confirmed through PCR with appropriate primer pairs. Generation of *Tal9b* mutant of PXO99^A
369 was generated in a similar manner using a 1252 bp fragment encoding a part of the DNA-
370 binding domain of the TALE for homology-based marker integration. All the primers used in
371 this study are listed in Table S3.

372 **Gene expression analysis**

373 Xoo and Xoc strains (wildtype and mutants) were cultured in PS broth for 24 hours at
374 28°C. The cells were pelleted by centrifugation at 4000xg for 10 minutes, washed with water
375 and adjusted to an optical density of 1.0 at 600nm with autoclaved water. The cell suspensions
376 or autoclaved water (mock) were syringe-infiltrated into 14 days-old TN1 leaves and further
377 incubated in the green house. Leaves around the site of infiltration (2cm) were collected 24
378 hours post infiltration, flash-frozen in liquid Nitrogen, and stored at -80°C until further
379 processing. For clip-inoculations, bacterial suspensions were processed as mentioned above
380 and fully expanded leaves of TN1 plants (50-60 days old) were cut with a scissor dipped in the
381 bacterial suspension. Leaf pieces of 1cm length were collected from the site of clipping at
382 different time points and stored at -80°C until further processing. RNA was isolated from the
383 leaves (8-10 leaves per treatment for infiltrated samples; 4-5 leaf pieces from clip-inoculated
384 samples) using RNeasy Plant Mini Kit (Qiagen, Germany). Depending on the RNA
385 concentration, about 1µg to 5µg total RNA was used for first-strand synthesis using RNA to
386 cDNA EcoDry Premix with Oligo(dT) (Takara Bio Inc., Japan), by following the
387 manufacturer's recommendations. cDNA was diluted to an RNA-equivalent concentration of
388 20-25ng/µl using nuclease-free water. Quantitative real-time PCR (qRT-PCR) reactions were
389 performed using 1ul diluted cDNA as template and 2X *Power SYBR*™ Green PCR Master
390 Mix (Applied Biosystems, US) in a 10µl reaction with 0.5µM forward and reverse primers
391 each. The reactions were performed on a ViiA 7 Real-Time PCR System (Applied Biosystems,

392 US) or CFX384 Touch RT-PCR detection system (Bio-Rad, US). *OsGAPDH*
393 (*LOC_Os04g40950.1*) was used as the internal control for expression normalisation. Relative
394 fold change values were calculated using the $2^{-\Delta\Delta CT}$ method (Livak and Schmittgen, 2001). For
395 semi-quantitative PCR, a 20 μ l reaction containing 2X KAPA Taq ReadyMix (Roche Applied
396 Sciences, Germany), 0.5 μ M forward and reverse primers specific to the transcript
397 variants/*OsGAPDH* and 1 μ l cDNA template (20ng/ μ l RNA-equivalent) was set and cycled 20
398 or 25 times. The reactions were then resolved in a 2% agarose gel and documented.

399 **Xoo virulence assay**

400 Xoo strains were cultured and processed as described above and the cell suspensions
401 were used to inoculate fully expanded leaves of 60-days old TN1 rice plants using the clip-
402 inoculation method with a scissor dipped in bacterial suspension (Kauffman et al., 1973).
403 Lesion lengths were measured at 14 days post inoculation from the site of clipping to the
404 leading edge of the disease lesion (dpi).

405 ***in silico* analyses**

406 The EBE sequence and its corresponding TAL effector was predicted using the
407 daTALbase server (Pérez-Quintero et al., 2018). The RVD sequences and classes of all the Xoo
408 and Xoc TAL effectors were retrieved using the “*Load and View TALE classes*” function of
409 the AnnoTALE tool (Grau et al., 2016). For the sequence homology analysis of
410 *LOC_Os03g03034.1*, all the known DMR6 homologues were identified and retrieved from
411 corresponding publications. The FNS, F2H, and F3H sequences were obtained from Li et al.,
412 2020. Where required, the homologous sequences were obtained using NCBI BLASTp
413 function with *LOC_Os03g03034.1* sequence as query. Phylogenetic analysis of the protein
414 sequences was conducted using the *Phylogeny.fr* server using default settings (Dereeper et al.,
415 2008) and the tree was visualised and annotated using the iTOL server (Letunic and Bork,
416 2021). All the sequences used for the phylogenetic analysis are provided in Data S1.

417 **Cloning *OsS5H/FNS-03g* for plant and biochemical experiments**

418 The coding sequence of *LOC_Os03g03034.1* was amplified from rice cDNA and
419 cloned into the Gateway-compatible entry vector pENTR/D-TOPO (Invitrogen, US) and
420 sequence verified. Further, the gene was sub-cloned into the Gateway destination vector
421 pH7FWG2 using LR Clonase II enzyme mix (Invitrogen, US) to generate the overexpression
422 (CaMV 35S promoter) expression clone with C-terminally fused eGFP. For recombinant
423 protein expression, the CDS of *LOC_Os03g03034.1* was cloned into pETM-40 using
424 restriction-free cloning (van den Ent and Löwe, 2006) to generate a reading frame comprising
425 *Maltose Binding Protein (MBP)*, *LOC_Os03g03034.1*, and *6X Histidine* coding sequences.

426 **Generation of *Arabidopsis* transgenics and *Pseudomonas syringae* infection assay**

427 *A. tumefaciens* AGL1 carrying the pH7FWG2:*Os03g03034.1* construct was cultured
428 overnight with appropriate antibiotics. An overnight grown, 250ml *Agrobacterial* culture was
429 centrifuged at 4000xg for 10 minutes, washed with water, and resuspended in 250ml floral-dip
430 solution (½ strength MS, 5% sucrose, 0.01% Silwet L-77). Developing inflorescence of
431 *Arabidopsis thaliana atdmr6* plants were dipped into the bacterial suspension for 2 minutes
432 and kept under high humidity for 24 hours and were maintained until seed collection at 22°C
433 and 16-hour photoperiod (Clough and Bent, 1998). The collected T₀ seeds were surface
434 sterilised for 20 minutes in 70% ethyl alcohol, stratified at 4°C for 48 hours, and plated on MS
435 agar plates containing appropriate selection (Phosphinothricin and Hygromycin). The selected
436 plants were further transferred to soil and grown for genotyping and collecting T₁ seeds. The
437 collected seeds were grown on selection plates for further experiments. The primers used for
438 genotyping the mutant plants and transgenics are listed in Table S3. Expression of
439 *Os03g03034*-GFP in the transgenic leaves was confirmed through immunoblotting using an
440 anti-GFP antibody (Abcam ab6556; 1:3000 dilution) and HRP-conjugated anti-rabbit
441 secondary antibody (Sigma 12-348; 1:50,000 dilution) (Figure S7). Freshly grown Pst DC3000

442 cells were resuspended in autoclaved water and adjusted to an OD₆₀₀ of 0.02. The cell
443 suspension was syringe-infiltrated into the fully expanded rosette leaves of Col-0, *atdmr6*, and
444 *atdmr6/Os03g03034-gfp* and maintained at 22°C and 16-hour photoperiod under high
445 humidity. The bacterial population was quantified at 0 dpi and 2 dpi by serial dilution plating
446 and counting the number of colony forming units per ml (cfu/ml) leaf extract.

447 **Recombinant protein purification**

448 The plasmids pETM-40 and pETM-40:*Os03g03034.1* were mobilised into *E. coli*
449 Rosetta DE3 cells. Both the clones were cultured at 37°C to an optical density of 0.4-0.6 at
450 600nm and the protein expression was induced by adding 0.5mM Isopropyl β-D-1-
451 thiogalactopyranoside (IPTG). The induced cultures were further grown at 18°C and 200rpm
452 for 16-20 hours. The proteins were purified using the amylose resin affinity purification method
453 by following the manufacturer's recommendations (E8021L, NEB). Briefly, about 1.5mL
454 slurry was used for purifying proteins from a 250mL culture. The induced cells were pelleted
455 at 4000xg for 20 minutes and the pellet was resuspended in 10mL lysis buffer (20mM Tris-
456 HCl (pH 7.4), 1mM EDTA, 200mM NaCl, 1mM PMSF, 1X protease inhibitor cocktail, 1mg/ml
457 Lysozyme, 1mM dithiothreitol). The cell suspension was sonicated at 30% amplitude for 20-
458 30 minutes with 10 sec on-off cycles. The lysate was clarified by centrifugation at max speed
459 for ~30 minutes. The supernatant was mixed with equilibrated resin and was gently mixed for
460 3 hours at 4°C and 10rpm in a rotator. The unbound fraction was collected by spinning the tubes
461 at 100xg for 1-2 minutes. The beads were washed with 5 bead volumes of wash buffer (20mM
462 Tris-HCl (pH 7.4), 1mM EDTA, 200mM NaCl) five times. The protein elution was performed
463 with 2 ml elution buffer (wash buffer+10mM maltose) each 3 to 4 times. Washing and elution
464 were performed by incubating the beads in corresponding buffers for 5-10 minutes at 4°C and
465 RT, respectively. All the fractions were resolved on an SDS-PAGE to assess protein recovery
466 and purity. Protein samples were dialyzed against dialysis buffer (50mM Tris (pH 7.4), 100mM

467 KCl, 1mM DTT, 30% Glycerol) 7 times and concentrated to a volume of ~600ul using Amicon
468 Ultra-155 centrifugal filters with MW cut-off of 30kDa. Protein quantity was measured using
469 NanoDrop Lite (Thermo Scientific, US). The concentrated samples were stored at -30°C until
470 further experiments.

471 **Biochemical assay for S5H activity**

472 The biochemical assay to test the SA hydroxylation activity of the protein was
473 performed as described earlier (Thomazella et al., 2021). Briefly, 60 μ g purified protein (MBP
474 and MBP-OsS5H/FNS-03g) was incubated in a 200 μ l reaction mixture at 40°C for 1-hour
475 (50mM 2-(N-morpholino) ethanesulfonic acid (MES; pH 6.5), 1mM α -ketoglutarate, 10mM
476 ascorbic acid, 0.4mM ferrous sulphate, 7.2 μ M salicylic acid) and later filtered through 0.22 μ m
477 filters. The filtered reaction mixture (10 μ l) was passed through a Zorbax SB C18 reverse phase
478 column (4.6mm x 25cm), 5um pore size at a flow rate of 0.75ml/min for a run time of 35
479 minutes per sample in a Thermo Vanquish UHPLC system. The column was first equilibrated
480 with 100% methanol. The mobile phase used for the run includes A: 0.2M sodium acetate (pH
481 5.5) and B: 100% methanol. The run condition is as follows: A:97%-B:3% for 15 minutes,
482 followed by A:93%-B:7% for 15 minutes, followed by A:97%-B:3% for 5 minutes. Authentic
483 standards of SA (#247588; Sigma, USA) and 2,5-DHBA (#149357; Sigma, USA) were
484 dissolved in 100% dimethyl formamide (DMF) at the required concentration (~7.2 μ M). SA
485 was detected at 403nm, while 2,5-DHBA was detected at 438nm, using a fluorescence detector.
486 The retention time of SA was observed to be ~24 minutes and that of 2,5-DHBA was ~11
487 minutes.

488 **Biochemical assay for FNS activity**

489 The biochemical assay to test the FNS activity of the protein was performed as follows:
490 100 μ g purified protein (MBP and MBP-OsS5H/FNS-03g) was incubated in a 200 μ l reaction
491 mixture at 30°C for 1 hour (50mM Tris (pH 7), 160 μ M α -ketoglutarate, 1mM ascorbic acid,

492 100 μ M ferrous sulphate, 200 μ M naringenin) and filtered through 0.22 μ m filters. The filtered
493 reaction mixture (50 μ l) was resolved on a Thermo Dionex UltiMate 3000 system using a
494 Zorbax SB C18 reverse phase column (4.6mm x 25cm), 5um pore size at a flow rate of
495 0.5ml/min for a run time of 1 hour per sample. The column was first equilibrated with 100%
496 methanol. The mobile phase used for the run includes A: 80% 10mM Ammonium acetate (pH
497 5.6): 20% Methanol and B: 100% methanol. The flow was set to 0% B for 2 minutes and 0 to
498 100% B in 50 minutes followed by 100% to 0% B in 3 minutes and continued at B 0% for 5
499 minutes. Authentic standards of Naringenin (#N5893; Sigma, USA) and Apigenin (#10798;
500 Sigma, USA) were dissolved in 100% DMF at the required concentration (~27 μ M). Naringenin
501 and apigenin were detected at 292nm and 340nm, respectively, using a UV detector. The
502 retention time of naringenin was observed to be ~33 minutes and that of apigenin was ~38
503 minutes.

504 Fractions corresponding to naringenin and apigenin retention times were collected
505 using a Thermo Scientific Fraction Collector and vacuum dried using Concentrator Plus
506 (Eppendorf, Germany). Dried fractions were resuspended in x μ l of 70% acetonitrile with 0.1%
507 trifluoroacetic acid. 1 μ l of the sample and 1 μ l of 10 mg/ml CHCA (α -Cyano-hydroxycinnamic
508 acid) matrix in 70% acetonitrile with 0.1% trifluoroacetic acid were mixed and spotted on a
509 MALDI plate and air-dried. The electrospray ionization (ESI) was performed in positive ion
510 mode. Mass spectra were acquired over a mass range of m/z 200-400. MALDI-TOF spectra
511 were acquired using a Spiral TOF JMS-S3000 (JEOL, Japan) Mass Spectrometer.

512 **Chemical treatment to assess *Xoo* virulence and gene expression levels**

513 Fully expanded leaves of 60 days-old TN1 plants were sprayed with 10 μ M apigenin (in
514 water and 0.05% Tween-20) or autoclaved water alone (with the appropriate amount of DMF
515 and 0.05% Tween-20) until run-off and grown in a green-house for 24 hours. Later, the leaves

516 were clip inoculated with the wild type or mutant strains of Xoo using the clip-inoculation
517 method and the lesion length was measured as described earlier.

518 Treatment with SA and naringenin was performed by incubating detached leaf pieces
519 (1cm²) from 50-60 days old TN1 plants on solutions containing 1mM SA or 0.5mM naringenin
520 or solvent control (mock). The stock solutions were prepared in absolute methanol and diluted
521 to the required concentration in autoclaved Milli-Q water with 0.01% SilwetTM L-77
522 (Momentive, NY, USA). The leaf pieces were collected at 1 hour, 6 hours, 12 hours, and 24
523 hours post-treatment, flash frozen, and stored at -80°C until further processing.

524 **Statistical analysis**

525 The data generated in this study were analysed using appropriate statistical methods,
526 wherever necessary, and the details are provided in the corresponding figure legends.

527 **Accession numbers**

528 OsS5H/FNS-03g - LOC_Os03g03034; OsGAPDH - LOC_Os04g40950; OsSWEET11
529 - LOC_Os08g42350; OsTFX1 - LOC_Os09g29820; hrcC (PXO99^A) - PXO_RS00410; Tal9b
530 (PXO99^A) - PXO_RS02485; hrcC (BXOR1) - ACU15_01175; AtDMR6 - AT5G24530.
531 *atdmr6* mutant plant - SK19087.

532 **ACKNOWLEDGEMENTS**

533 This study was supported by the grants provided to HKP from the Council of Scientific and
534 Industrial Research, New Delhi, India (MLP0121 Phase-I and II) and to RVS from the Science
535 and Engineering Research Board (SERB), Department of Science and Technology,
536 Government of India (SB/S2/JCB-12/2014). GCG, SD, NG, AM, NG, RPR, and NS thank the
537 Council for Scientific and Industrial Research for their fellowships. DJ thanks the Department
538 of Biotechnology, New Delhi, India for granting their Research Associateship.

539 **DATA AVAILABILITY STATEMENT**

540 Information on publicly available data analysed in this study is provided in the supplementary
541 information of this article. All other data generated for this study are present in the main text
542 or supplementary information. The materials from this study can be obtained from the
543 corresponding author upon reasonable request.

544

545 **REFERENCES**

546 An, J., Kim, Sun Ho, Bahk, S., Vuong, U.T., Nguyen, N.T., Do, H.L., et al. (2021) Naringenin
547 Induces Pathogen Resistance Against *Pseudomonas syringae* Through the Activation
548 of NPR1 in *Arabidopsis*. *Frontiers in Plant Science*, 12, 672552.
549 <https://doi.org/10.3389/fpls.2021.672552>.

550 Antony, G., Zhou, J., Huang, S., Li, T., Liu, B., White, F., et al. (2010) Rice xa13 recessive
551 resistance to bacterial blight is defeated by induction of the disease susceptibility gene
552 Os-11N3. *Plant Cell*, 22, 3864–3876. <https://doi.org/10.1105/tpc.110.078964>.

553 Bezrutczyk, M., Yang, J., Eom, J.-S., Prior, M., Sosso, D., Hartwig, T., et al. (2018) Sugar flux
554 and signaling in plant-microbe interactions. *The Plant Journal: For Cell and Molecular
555 Biology*, 93, 675–685. <https://doi.org/10.1111/tpj.13775>.

556 Blanvillain-Baufumé, S., Reschke, M., Solé, M., Auguy, F., Doucoure, H., Szurek, B., et al.
557 (2017) Targeted promoter editing for rice resistance to *Xanthomonas oryzae* pv. *oryzae*
558 reveals differential activities for SWEET14-inducing TAL effectors. *Plant
559 Biotechnology Journal*, 15, 306–317. <https://doi.org/10.1111/pbi.12613>.

560 Boch, J., Scholze, H., Schornack, S., Landgraf, A., Hahn, S., Kay, S., et al. (2009) Breaking
561 the code of DNA binding specificity of TAL-type III effectors. *Science*, 326, 1509–
562 1512. <https://doi.org/10.1126/science.1178811>.

563 Bogdanove, A.J., Schornack, S. & Lahaye, T. (2010) TAL effectors: Finding plant genes for
564 disease and defense. *Current Opinion in Plant Biology*, 13, 394–401.
565 <https://doi.org/10.1016/j.pbi.2010.04.010>.

566 Cai, L., Cao, Y., Xu, Z., Ma, W., Zakria, M., Zou, L., et al. (2017) A Transcription Activator-
567 Like Effector Tal7 of *Xanthomonas oryzae* pv. *Oryzicola* Activates Rice Gene
568 Os09g29100 to Suppress Rice Immunity. *Scientific Reports*, 7, 1–13.
569 <https://doi.org/10.1038/s41598-017-04800-8>.

570 Casas, M.I., Duarte, S., Doseff, A.I. & Grotewold, E. (2014) Flavone-rich maize: an
571 opportunity to improve the nutritional value of an important commodity crop. *Frontiers
572 in Plant Science*, 5.

573 Cernadas, R.A., Doyle, E.L., Niño-Liu, D.O., Wilkins, K.E., Bancroft, T., Wang, L., et al.
574 (2014) Code-assisted discovery of TAL effector targets in bacterial leaf streak of rice
575 reveals contrast with bacterial blight and a novel susceptibility gene. *PLoS pathogens*,
576 10, e1003972. <https://doi.org/10.1371/journal.ppat.1003972>.

577 Chu, Z., Fu, B., Yang, H., Xu, C., Li, Z., Sanchez, A., et al. (2006) Targeting xa13, a recessive
578 gene for bacterial blight resistance in rice. *Theoretical and Applied Genetics*, 112, 455–
579 461. <https://doi.org/10.1007/s00122-005-0145-6>.

580 Clough, S.J. & Bent, A.F. (1998) Floral dip: a simplified method for Agrobacterium-mediated
581 transformation of *Arabidopsis thaliana*. *The Plant Journal: For Cell and Molecular
582 Biology*, 16, 735–743. <https://doi.org/10.1046/j.1365-313x.1998.00343.x>.

583 Dereeper, A., Guignon, V., Blanc, G., Audic, S., Buffet, S., Chevenet, F., et al. (2008)
584 Phylogeny.fr: robust phylogenetic analysis for the non-specialist. *Nucleic Acids*
585 *Research*, 36, W465-469. <https://doi.org/10.1093/nar/gkn180>.

586 Djennane, S., Gersch, S., Le-Bohec, F., Piron, M.-C., Baltenweck, R., Lemaire, O., et al. (2023)
587 Reduced susceptibility to downy mildew in grapevine plants edited for VvDMR6-1.
588 *Journal of Experimental Botany*, *erad487*. <https://doi.org/10.1093/jxb/erad487>.

589 Ent, F. van den & Löwe, J. (2006) RF cloning: a restriction-free method for inserting target
590 genes into plasmids. *Journal of Biochemical and Biophysical Methods*, 67, 67–74.
591 <https://doi.org/10.1016/j.jbbm.2005.12.008>.

592 Falcone Ferreyra, M.L., Emiliani, J., Rodriguez, E.J., Campos-Bermudez, V.A., Grotewold, E.
593 & Casati, P. (2015) The Identification of Maize and Arabidopsis Type I FLAVONE
594 SYNTHASEs Links Flavones with Hormones and Biotic Interactions. *Plant*
595 *Physiology*, 169, 1090–1107. <https://doi.org/10.1104/pp.15.00515>.

596 Fukagawa, N.K. & Ziska, L.H. (2019) Rice: Importance for Global Nutrition. *Journal of*
597 *Nutritional Science and Vitaminology*, 65, S2–S3. <https://doi.org/10.3177/jnsv.65.S2>.

598 Grau, J., Reschke, M., Erkes, A., Streubel, J., Morgan, R.D., Wilson, G.G., et al. (2016)
599 AnnoTALE: bioinformatics tools for identification, annotation and nomenclature of
600 TALEs from *Xanthomonas* genomic sequences. *Scientific Reports*, 6, 21077.
601 <https://doi.org/10.1038/srep21077>.

602 Hasley, J.A.R., Navet, N. & Tian, M. (2021) CRISPR/Cas9-mediated mutagenesis of sweet
603 basil candidate susceptibility gene ObDMR6 enhances downy mildew resistance
604 Varshney, G. (Ed.). *PLOS ONE*, 16, e0253245.
605 <https://doi.org/10.1371/journal.pone.0253245>.

606 Kauffman, H.E., Reddy, A.P.K., Hsieh, S.P.Y. & Merca, S.D. (1973) An improved technique
607 for evaluating resistance of rice varieties to *Xanthomonas oryzae*. *Plant Dis. Rep.*, 57,
608 737–741.

609 Kim, J.H., Cheon, Y.M., Kim, B.-G. & Ahn, J.-H. (2008) Analysis of flavonoids and
610 characterization of theOsFNS gene involved in flavone biosynthesis in Rice. *Journal*
611 *of Plant Biology*, 51, 97–101. <https://doi.org/10.1007/BF03030717>.

612 Kumar, S., Stecher, G., Li, M., Knyaz, C. & Tamura, K. (2018) MEGA X: Molecular
613 Evolutionary Genetics Analysis across Computing Platforms. *Molecular Biology and*
614 *Evolution*, 35, 1547–1549. <https://doi.org/10.1093/molbev/msy096>.

615 Letunic, I. & Bork, P. (2021) Interactive Tree Of Life (iTOL) v5: an online tool for
616 phylogenetic tree display and annotation. *Nucleic Acids Research*, 49, W293–W296.
617 <https://doi.org/10.1093/NAR/GKAB301>.

618 Li, D.-D., Ni, R., Wang, P.-P., Zhang, X.-S., Wang, P.-Y., Zhu, T.-T., et al. (2020) Molecular
619 Basis for Chemical Evolution of Flavones to Flavonols and Anthocyanins in Land
620 Plants. *Plant Physiology*, 184, 1731–1743. <https://doi.org/10.1104/pp.20.01185>.

621 Liu, X., Yu, Y., Yao, W., Yin, Z., Wang, Y., Huang, Z., et al. (2023) CRISPR/Cas9-mediated
622 simultaneous mutation of three salicylic acid 5-hydroxylase (OsS5H) genes confers

623 broad-spectrum disease resistance in rice. *Plant Biotechnology Journal*, 21, 1873–
624 1886. <https://doi.org/10.1111/pbi.14099>.

625 Livak, K.J. & Schmittgen, T.D. (2001) Analysis of relative gene expression data using real-
626 time quantitative PCR and the 2(-Delta Delta C(T)) Method. *Methods (San Diego, Calif.)*, 25, 402–408. <https://doi.org/10.1006/meth.2001.1262>.

628 Mansueto, L., Fuentes, R.R., Borja, F.N., Detras, J., Abrio-Santos, J.M., Chebotarov, D., et al.
629 (2017) Rice SNP-seek database update: new SNPs, indels, and queries. *Nucleic Acids Research*, 45, D1075–D1081. <https://doi.org/10.1093/NAR/GKW1135>.

631 Mücke, S., Reschke, M., Erkes, A., Schwietzer, C.-A., Becker, S., Streubel, J., et al. (2019)
632 Transcriptional Reprogramming of Rice Cells by *Xanthomonas oryzae* TALEs.
633 *Frontiers in Plant Science*, 10.

634 Niño-Liu, D.O., Ronald, P.C. & Bogdanove, A.J. (2006) *Xanthomonas oryzae* pathovars:
635 model pathogens of a model crop. *Molecular Plant Pathology*, 7, 303–324.
636 <https://doi.org/10.1111/J.1364-3703.2006.00344.X>.

637 Oliva, R., Ji, C., Atienza-Grande, G., Huguet-Tapia, J.C., Perez-Quintero, A., Li, T., et al.
638 (2019) Broad-spectrum resistance to bacterial blight in rice using genome editing.
639 *Nature Biotechnology*, 37, 1344–1350. <https://doi.org/10.1038/s41587-019-0267-z>.

640 Padmavati, M., Sakthivel, N., Thara, K.V. & Reddy, A.R. (1997) Differential sensitivity of rice
641 pathogens to growth inhibition by flavonoids. *Phytochemistry*, 46, 499–502.
642 [https://doi.org/10.1016/S0031-9422\(97\)00325-7](https://doi.org/10.1016/S0031-9422(97)00325-7).

643 Peng, Z., Hu, Y., Zhang, J., Huguet-Tapia, J.C., Block, A.K., Park, S., et al. (2019)
644 *Xanthomonas translucens* commandeers the host rate-limiting step in ABA
645 biosynthesis for disease susceptibility. *Proceedings of the National Academy of
646 Sciences*, 116, 20938–20946. <https://doi.org/10.1073/pnas.1911660116>.

647 Pérez-Quintero, A.L., Lamy, L., Zarate, C.A., Cunnac, S., Doyle, E., Bogdanove, A., et al.
648 (2018) daTALbase: A Database for Genomic and Transcriptomic Data Related to TAL
649 Effectors. *Molecular Plant-Microbe Interactions®*, 31, 471–480.
650 <https://doi.org/10.1094/MPMI-06-17-0153-FI>.

651 Peters, N.K., Frost, J.W. & Long, S.R. (1986) A Plant Flavone, Luteolin, Induces Expression
652 of *Rhizobium meliloti* Nodulation Genes. *Science*, 233, 977–980.
653 <https://doi.org/10.1126/science.3738520>.

654 Pirrello, C., Malacarne, G., Moretto, M., Lenzi, L., Perazzolli, M., Zeilmaker, T., et al. (2022)
655 Grapevine DMR6-1 Is a Candidate Gene for Susceptibility to Downy Mildew.
656 *Biomolecules*, 12, 182. <https://doi.org/10.3390/biom12020182>.

657 Pucker, B. & Iorizzo, M. (2023) Apiaceae FNS I originated from F3H through tandem gene
658 duplication. *PloS One*, 18, e0280155. <https://doi.org/10.1371/journal.pone.0280155>.

659 Righini, S., Rodriguez, E.J., Berosich, C., Grotewold, E., Casati, P. & Falcone Ferreyra, M.L.
660 (2019) Apigenin produced by maize flavone synthase I and II protects plants against
661 UV-B-induced damage. *Plant, Cell & Environment*, 42, 495–508.
662 <https://doi.org/10.1111/pce.13428>.

663 Salzberg, S.L., Sommer, D.D., Schatz, M.C., Phillippy, A.M., Rabinowicz, P.D., Tsuge, S., et
664 al. (2008) Genome sequence and rapid evolution of the rice pathogen *Xanthomonas*
665 *oryzae* pv. *oryzae* PXO99A. *BMC Genomics*, 9, 204. <https://doi.org/10.1186/1471-2164-9-204>.

667 Savary, S., Willocquet, L., Pethybridge, S.J., Esker, P., McRoberts, N. & Nelson, A. (2019)
668 The global burden of pathogens and pests on major food crops. *Nature Ecology and*
669 *Evolution*, 3, 430–439. <https://doi.org/10.1038/s41559-018-0793-y>.

670 Shi, H., Jiang, J., Yu, W., Cheng, Y., Wu, S., Zong, H., et al. (2024) Naringenin restricts the
671 colonization and growth of *Ralstonia solanacearum* in tobacco mutant KCB-1. *Plant*
672 *Physiology*, kiae185. <https://doi.org/10.1093/plphys/kiae185>.

673 Streubel, J., Pesce, C., Hutin, M., Koebnik, R., Boch, J. & Szurek, B. (2013) Five
674 phylogenetically close rice SWEET genes confer TAL effector-mediated susceptibility
675 to *Xanthomonas oryzae* pv. *oryzae*. *The New Phytologist*, 200, 808–819.
676 <https://doi.org/10.1111/nph.12411>.

677 Sugio, A., Yang, B., Zhu, T. & White, F.F. (2007) Two type III effector genes of *Xanthomonas*
678 *oryzae* pv. *oryzae* control the induction of the host genes *OsTFIIA γ 1* and *OsTFX1*
679 during bacterial blight of rice. *Proceedings of the National Academy of Sciences*, 104,
680 10720–10725. <https://doi.org/10.1073/pnas.0701742104>.

681 Sun, M., Li, L., Wang, C., Wang, L., Lu, D., Shen, D., et al. (2022) Naringenin confers defence
682 against *Phytophthora nicotianae* through antimicrobial activity and induction of
683 pathogen resistance in tobacco. *Molecular Plant Pathology*, 23, 1737–1750.
684 <https://doi.org/10.1111/mpp.13255>.

685 Thomazella, D.P. de T., Seong, K., Mackelprang, R., Dahlbeck, D., Geng, Y., Gill, U.S., et al.
686 (2021) Loss of function of a DMR6 ortholog in tomato confers broad-spectrum disease
687 resistance. *Proceedings of the National Academy of Sciences of the United States of*
688 *America*, 118, e2026152118. <https://doi.org/10.1073/pnas.2026152118>.

689 Tran, T.T., Pérez-Quintero, A.L., Wonni, I., Carpenter, S.C.D., Yu, Y., Wang, L., et al. (2018)
690 Functional analysis of African *Xanthomonas oryzae* pv. *oryzae* TALomes reveals a new
691 susceptibility gene in bacterial leaf blight of rice. *PLoS pathogens*, 14, e1007092.
692 <https://doi.org/10.1371/journal.ppat.1007092>.

693 Van Damme, M., Huibers, R.P., Elberse, J. & Van Den Ackerveken, G. (2008) *Arabidopsis*
694 *DMR6* encodes a putative 2OG-Fe(II) oxygenase that is defense-associated but required
695 for susceptibility to downy mildew. *The Plant Journal*, 54, 785–793.
696 <https://doi.org/10.1111/j.1365-313X.2008.03427.x>.

697 Wang, Yan & Wang, Yuanchao (2018) Trick or Treat: Microbial Pathogens Evolved
698 Apoplastic Effectors Modulating Plant Susceptibility to Infection. *Molecular Plant-Microbe*
699 *Interactions*®, 31, 6–12. <https://doi.org/10.1094/MPMI-07-17-0177-FI>.

700 Watson, B.S., Bedair, M.F., Urbanczyk-Wojniak, E., Huhman, D.V., Yang, D.S., Allen, S.N.,
701 et al. (2015) Integrated metabolomics and transcriptomics reveal enhanced specialized
702 metabolism in *Medicago truncatula* root border cells. *Plant Physiology*, 167, 1699–
703 1716. <https://doi.org/10.1104/pp.114.253054>.

704 White, F., Potnis, N., Jones, J.B. & Koebnik, R. (2009) The type III effectors of *Xanthomonas*.
705 *Molecular Plant Pathology*, 10, 749–766. <https://doi.org/10.1111/j.1364-3703.2009.00590.x>.

707 Wu, T., Zhang, H., Yuan, B., Liu, H., Kong, L., Chu, Z., et al. (2022) Tal2b targets and activates
708 the expression of OsF3H03g to hijack OsUGT74H4 and synergistically interfere with
709 rice immunity. *New Phytologist*, 233, 1864–1880. <https://doi.org/10.1111/nph.17877>.

710 Yan, D., Tajima, H., Cline, L.C., Fong, R.Y., Ottaviani, J.I., Shapiro, H.-Y., et al. (2022)
711 Genetic modification of flavone biosynthesis in rice enhances biofilm formation of soil
712 diazotrophic bacteria and biological nitrogen fixation. *Plant Biotechnology Journal*, 20,
713 2135–2148. <https://doi.org/10.1111/pbi.13894>.

714 Yang, B., Sugio, A. & White, F.F. (2006) Os8N3 is a host disease-susceptibility gene for
715 bacterial blight of rice. *Proc Natl Acad Sci U S A*, 103, 10503–10508.
716 <https://doi.org/10.1073/pnas.0604088103>.

717 Yang, Z., Li, N., Kitano, T., Li, P., Spindel, J.E., Wang, L., et al. (2021) Genetic mapping
718 identifies a rice naringenin O-glucosyltransferase that influences insect resistance. *The*
719 *Plant Journal*, 106, 1401–1413. <https://doi.org/10.1111/tpj.15244>.

720 Yu, P., He, X., Baer, M., Beirinckx, S., Tian, T., Moya, Y.A.T., et al. (2021) Plant flavones
721 enrich rhizosphere Oxalobacteraceae to improve maize performance under nitrogen
722 deprivation. *Nature Plants*, 7, 481–499. <https://doi.org/10.1038/s41477-021-00897-y>.

723 Zeilmaker, T., Ludwig, N.R., Elberse, J., Seidl, M.F., Berke, L., Van Doorn, A., et al. (2015)
724 DOWNY MILDEW RESISTANT 6 and DMR 6- LIKE OXYGENASE 1 are partially
725 redundant but distinct suppressors of immunity in *Arabidopsis*. *The Plant Journal*, 81,
726 210–222. <https://doi.org/10.1111/tpj.12719>.

727 Zhang, H., Zhang, F., Yu, Y., Feng, L., Jia, J., Liu, B., et al. (2020) A Comprehensive Online
728 Database for Exploring ~20,000 Public *Arabidopsis* RNA-Seq Libraries. *Molecular*
729 *Plant*, 13, 1231–1233. <https://doi.org/10.1016/j.molp.2020.08.001>.

730 Zhang, Y., Yu, Q., Gao, S., Yu, N., Zhao, L., Wang, J., et al. (2022) Disruption of the primary
731 salicylic acid hydroxylases in rice enhances broad-spectrum resistance against
732 pathogens. *Plant, Cell & Environment*, 45, 2211–2225.
733 <https://doi.org/10.1111/pce.14328>.

734 Zhang, Y., Zhao, L., Zhao, J., Li, Y., Wang, J., Guo, R., et al. (2017) *S5H/DMR6* Encodes a
735 Salicylic Acid 5-Hydroxylase That Fine-Tunes Salicylic Acid Homeostasis. *Plant*
736 *Physiology*, 175, 1082–1093. <https://doi.org/10.1104/pp.17.00695>.

737 Zhu, Y.-X., Ge, C., Ma, S., Liu, X.-Y., Liu, M., Sun, Y., et al. (2020) Maize ZmFNSI Homologs
738 Interact with an NLR Protein to Modulate Hypersensitive Response. *International*
739 *Journal of Molecular Sciences*, 21, 2529. <https://doi.org/10.3390/ijms21072529>.

740

741 **CONFLICT OF INTEREST**

742 The authors declare no conflict of interests.

743 **AUTHOR CONTRIBUTION**

744 Conceptualisation - GCG, SD, and HKP. Investigation - GCG (computational and phylogenetic
745 analyses), GCG, SD, NG (bacterial mutagenesis, gene expression analysis, gene cloning for
746 plant expression, *Arabidopsis* complementation, pathogen infection assays); GCG, AM, GN
747 (recombinant protein purification); AM (biochemical activity assays, HPLC, and gene
748 expression analysis); NS (gene cloning for protein purification); RPR and DJ (plant
749 transformation). Assessment and supervision of the work - HKP and RVS. Writing of original
750 draft – GCG, SD, NG. Manuscript proofreading - all the authors. Funding acquisition – HKP
751 and RVS.